Matter and Radiation at Extremes | RESEARCH ARTICLE | scitation.org/journal/mre

Ion source perturbation and control in intense laser plasma interaction

Cite as: Matter Radiat. Extremes 5, 045402 (2020); doi: 10.1063/5.0004801
Submitted: 15 February 2020 • Accepted: 17 May 2020 •
Published Online: 1 June 2020

B. Ramakrishna,[1,a] S. Krishnamurthy,[1] M. Tayyab,[2,3] S. Bagchi,[2] K. Makur,[1] Raoul Trines,[4] Robbie Scott,[4] Alex Robinson,[4] and J. A. Chakera[2,3]

AFFILIATIONS

[1]Department of Physics, Indian Institute of Technology Hyderabad, Kandi, Sangareddy 502285, India
[2]Laser Plasma Division, Raja Ramanna Centre for Advanced Technology, Indore 452 013, India
[3]Homi Bhabha National Institute, Training School Complex, Anushakti Nagar, Mumbai 400094, India
[4]Central Laser Facility, STFC Rutherford-Appleton Laboratory, Didcot OX11 0QX, United Kingdom

[a]**Author to whom correspondence should be addressed:** bhuvan@iith.ac.in

ABSTRACT

We present here experimental results on the optimization of the mega-electronvolt ion source from the target front surface by using relativistic (10^{18} W/cm^2) interactions with ultra-short laser pulses (50 fs). The source perturbation in the accelerated proton/ion beam was primarily controlled by the addition of a pre-pulse to main pulse contrast ratio. The 2D particle-in-cell simulations agreed well with the observed experimental results for the ion source perturbation and mitigation. This work provides insights into ion source perturbations (temporal and spatial) and the need to control them in intense laser–plasma interactions. Our results may assist in the efficient guiding of proton/ion beams to the core of fusion fuel or of ions in cancer therapy.

I. INTRODUCTION

The acceleration of high-energy ion beams (up to several tens of mega-electronvolts per nucleon) following the interaction of ultra-short ($t < 1$ ps) and intense ($I\lambda^2 > 10^{18}$ W cm^{-2}) laser pulses with solid targets has been an active research area in the last few years. Mechanisms leading to forward-accelerated high-quality ion beams, operating at the currently accessible intensities in laser–matter interactions, are mainly associated with the large electric fields created by laser-accelerated electrons at the target interface. The emitted ion pulses contain many particles (up to 10^{13}) with energies in excess of several mega-electronvolts,[1] have about picosecond pulse duration,[2] and a source size of tens to hundreds of micrometers. In addition, conversion efficiencies (of laser energy to proton energy) of up to 7% have been reported.[3]

The above outstanding characteristics of laser-accelerated ion beams have triggered discussions about their application as an ion source injected into conventional particle accelerators.[4] At current intensity regimes, the charge separation fields created during this interaction with thin foils offer a far larger acceleration gradient (10^{12} V/m) than those achieved in conventional radio-frequency accelerator cavities (10^8 V/m). In fundamental research, laser-accelerated protons are successfully used for diagnosing fast-changing electromagnetic fields in laser-produced plasmas, with picosecond resolution.[5–7] Another application proposed for laser-driven proton or ion beams is in radiation therapy.[3] This would provide possibilities of better dose conformity to the treatment target compared to the commonly used photon or electron beams. Proton beams have a low entrance dose, rapid falloff at the edge of the dose distribution, and the maximum rate of energy loss at the end of the range, which is referred to as the *Bragg peak* effect.[8,9]

The unique properties of protons from high-intensity laser–matter interactions, particularly in terms of spatial quality and temporal duration, have opened up the totally new applications of proton probing and proton radiography.[10–14] These applications exploit the ultra-low emittance and high degree of laminarity of the source to achieve high spatial resolution when probing samples in a point projection backlighting scheme. It would also be useful to produce proton/ion beams with a limited energy spread, in contrast to the broad spectrum beams typically achieved in recent experiments.[15–17] In particular, high-quality beams with a small energy spread are required when spatially accurate energy deposition in a cancerous tissue is important.[9] Fast changes in the acceleration

sheath limit the use of proton beams in probing to the study of the ultra-fast dynamics at picosecond time scales. In this case, the velocity of the protons is a function of time from the point source, as a result of which the beam leaves the acceleration sheath with a velocity chirp. Such a velocity chirp is an important characteristic, as it sheds light on the temporal development of the acceleration. This velocity chirp of the accelerated protons was mentioned in the theoretical investigations by Cowan *et al.*[18]

Recent experiments[19] have reported a deviation in the proton emission characteristics at the highest energy from the target normal direction. This non-target normal emission of protons at higher energies has been ascribed to a fast-directed intra-pulse acceleration mechanism. There are very limited experimental details[20] describing this behavior of charged particles. Information about the proton spectrum could directly correlate with the information about the hot electron sheath evolving at an ultra-fast timescale. Experiments on tiny laser-irradiated water droplets, as used in Refs. 17, 21,22, gave, for all the ions, perfect parabolic traces on a Thomson parabola ion spectrograph (TPIS). This indicates that the geometry of the deflecting *B* and *E* fields of the spectrograph produces no artifacts in the ion trajectories. Further confirmation of this came from foil target experiments that had a 5° deviation of the proton-beam imprint recorded at high energies using a complementary detector for the ions i.e., radiochromic films.[17] This further confirms that the wiggling is mainly due to the fast changes in the accelerating sheath. To explain the ion acceleration and wiggling in solid CH foil targets, Tikhonchuk *et al.*[23] developed a two-species plasma model with a single isothermal electron population. The results pointed to the possibility of spectral control with the appropriate target conditions. In this paper, we report on the observation of wiggling in an accelerated proton beam as it traverses through a dense plasma sheath.

II. EXPERIMENTAL DETAILS

The experiments were carried out using a 10-TW Ti:sapphire laser system at the Raja Ramanna Centre for Advanced Technology, Indore, which delivered 50-fs (FWHM) 420-mJ pulses at a 10-Hz repetition rate at a central wavelength of 800 nm. The p-polarized laser beam was focused to a focal spot 10 μm in diameter (FWHM) by a gold-coated f/7.5 off-axis parabolic mirror to give a peak intensity of the order of ~2×10^{18} W/cm^2. A schematic diagram of the experimental setup is shown in Fig. 1.

The angle of incidence of the laser on the target was set to 45° to allow efficient absorption of the laser pulse.[3] The laser pre-pulse was monitored for each laser shot using a fast photodiode connected to a 1-GHz oscilloscope. The laser pulse had an amplified spontaneous emission (ASE) pedestal for about 2 ns before the main pulse. The intensity contrast ratio between the main pulse and the pedestal was about 10^6. Plastic/Mylar targets of 1 mm thickness were used in the experiment. A Thomson parabola ion spectrograph (TPIS) with an acceptance angle of 20° and a lead pinhole of diameter 200 μm was used to diagnose the ion beam along the normal of the target front surface. The field plates in the TPIS were 18 mm apart and 80 mm in length. A magnetic field of 0.85 kG and an electric field of 1.5 kV were applied between them. The ions were deflected by the parallel electric and magnetic fields according to their velocity and charge-to-mass ratio. The dispersed ion beam was detected by a micro-channel plate detector coupled to a 16-bit CCD camera (Andor, EMCCD).

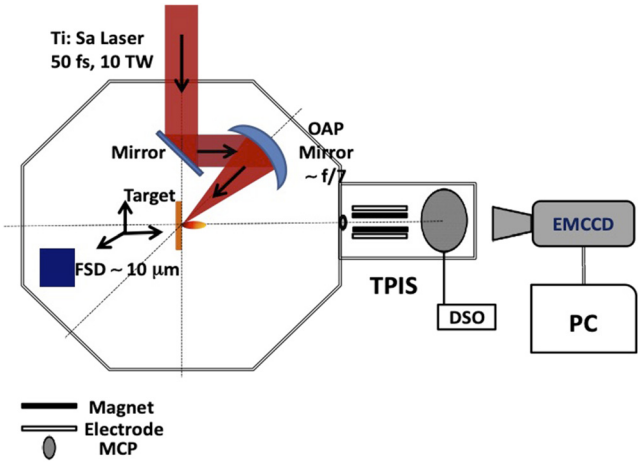

FIG. 1. Experimental setup. The laser (λ = 800 nm) was focused by an off-axis parabola (f/7.5) at an angle of 45° to the target. It produced up to 400 mJ in 45 fs with peak intensities ~2×10^{18} W cm^{-2}.

III. RESULTS AND DISCUSSION

Now we discuss the possibility of controlling the pointing of accelerated ion beams by adding a pre-pulse to the main pulse of the laser. The wiggling of the proton traces was studied in detail by varying the pre-pulse conditions, for Perspex [poly-(methylmethacrylate) or PMMA], Mylar (CH_n), and deuterated polyethylene (CD_2) targets, which are observed by the TPIS detector. Figure 2(a) shows wiggled proton traces observed using the TPIS for plain Perspex, Mylar, and CD_2 targets at the best focus of the laser beam. Figure 2(b) shows the same but with a pre-pulse added to the main laser pulse. Significant wiggling of the high-energy proton spectrum was recorded by the micro-channel plate, especially for the heavier carbon ions [Fig. 2(a)].

When the ASE pre-pulse was extended by changing the switch-out time of the pulse selector in the laser, the wiggling features in the spectral trace were considerably reduced, with no reduction in the maximum ion energy [Fig. 2(b)]. With the Mylar target, there was significant wiggling for heavier ions like carbon but not for protons. Robinson *et al.*[24] proposed a scheme to obtain spectral control of laser-accelerated protons using two intense collinear laser pulses. The first pulse (pre-pulse), lower in intensity by a factor of 10 than the second pulse, interacts with the target to create a channel of hot electrons, which results in an azimuthal magnetic field. The second laser pulse (the main pulse) creates hot electrons, which are guided through the channels already produced by the pre-pulse, thereby effectively decreasing the source instabilities in the proton beam. However, in our experiments, since the pre-pulse is very long, we did not observe a channeling effect.

The wiggling of the traces in our case could be attributed to the presence of multiple sources, which create perturbations in the accelerating sheath (in the absence of a pre-pulse). The pre-pulse wipes out the source multiplicity occurring at ps time scales. Thus, one can control the ion source perturbations in a laser plasma and mitigate the effects by varying the extent of the laser pulse. In other words, by using an extended pre-pulse, one can eliminate wiggling from the proton

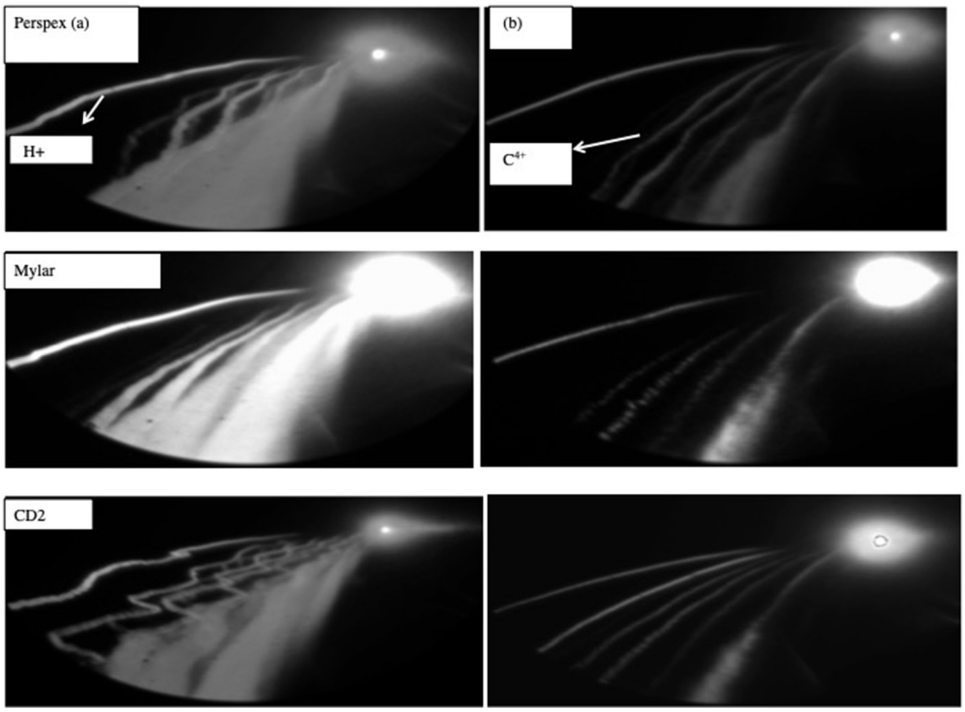

FIG. 2. Proton beam traces from the front surfaces of Perspex (top), Mylar (center), and CD_2 (bottom) targets. The images show the wiggling of the beam with the target at the best focus, (a) without a pre-pulse and (b) with a pre-pulse.

spectral trace. However, the wiggling of the heavier ion beams in our experiment could not be controlled very effectively using this technique, due to their slow response to the sheath field. Note that we used the same experimental and diagnostic conditions for experiments both with and without the laser pre-pulse, and our results confirm that there were no experimental artifacts due to the detector.

As reported in the literature,[5] target normal sheath acceleration protons have a typical divergence of 10°–20° with small emittance, and a source size ranging from 300 μm to 500 μm. The ion emission in the present experiment was observed from an extended area of the target of around ±200 μm relative to the target center. If the protons within the observed energy range are all emitted from the same source

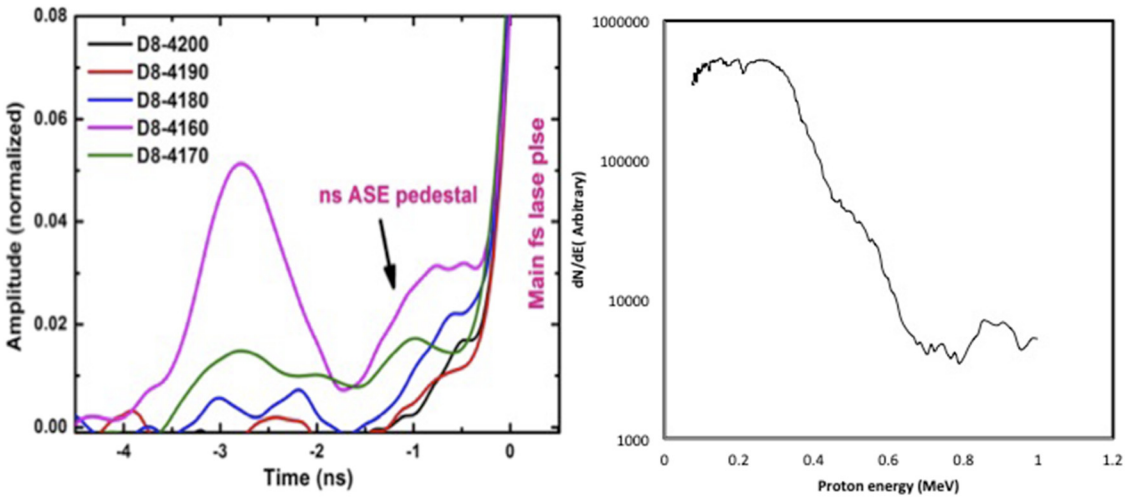

FIG. 3. (a) Laser pre-pulse contrast at various Pockels cell settings. (b) A typical proton (H^+) energy spectra recorded for a pre-pulse on a Perspex target showing the 1-MeV cutoff.

point, the projection of their spectrum should result in a smooth spectral trace, as observed in Fig. 2(b). Also, Fig. 2(b) shows that the heavy-ion beams do not overlap [unlike in Fig. 2(a)], which indicates that the source is highly laminar in nature when a pre-plasma is used. It also indicates that the high-energy ions are emitted from a smaller target region with lower divergence, and the low-energy ions have a larger (around a few mm) source size. The ASE pre-pulse level of the laser was monitored using a fast photodiode and a fast oscilloscope for each laser exposure. Figure 3(a) shows the level of ASE for the pre-pulse with the laser at different settings. In the normal configuration, the ASE pre-pulse to main pulse contrast ratio of 10^{-6} was maintained in the laser (D8-4200). To ensure that the wiggling features are not due to the pinhole aperture in front of the TPIS, we studied the interaction with two different pinhole diameters (200 μm and 300 μm).

The laser intensity and energy determine the pulse of the hot electrons circulating through the target and the building up of the acceleration sheath at the front of the target. As described previously, ions are accelerated by the electron sheath at the front. The spatial and angular characteristics are determined by the electron density distribution within the sheath. At higher energies, the proton beam has an angular distribution with a sharp boundary. The electron sheath follows a generic bell-shaped spatial distribution. The high-energy protons are accelerated from the tip of the sheath with a very small divergence angle. The acceleration of low-energy protons occurs from larger regions, including the wings of the sheath, and hence, a large divergence is observed. The virtual source position in front of the target changes for different proton energies, which implies that protons with different energies are emitted with an accelerating sheath field with a different curvature. In Ref. 20, this observation of wiggling from the rear of the target is explained using an imaging mode configuration (15:1). In our setup, we clearly observe this distinction from the front of the target without using any magnification.

IV. SIMULATIONS

Two-dimensional particle-in-cell (PIC) simulations were performed using the PIC code Osiris.[25] In these simulations, a powerful laser beam interacts with a CH foil, with a thickness of 10 μm and a radius of 30 μm. Two scenarios were considered: (1) a hard-edge (no pre-pulse) where the density profile along the target normal direction is simply a rectangle and (2) a gradient profile (with a pre-pulse) where the density profile has a linear gradient facing the laser beam. The motivation for these scenarios was as follows. In the experiment, the targets used were similar from shot to shot, but in some shots, the main laser pulse was preceded by a long pre-pulse (2 ns pedestal), while in other shots, this pre-pulse was absent. Hydrodynamic modeling indicates that the pre-pulse will heat up the target and create a plasma plume in front of the foil target, which expands thermally towards the laser pulse and forms a long density gradient. To simulate the pre-pulse case, we used an initial plasma density profile with a density gradient facing the laser pulse, to mimic the configuration in the experiment. In other simulations, we used an initial plasma density profile without a density gradient and only a hard edge facing the laser pulse, to mimic the configuration without a pre-pulse.

The numerical parameters were as follows. In the hard-edge simulations, the simulation box measures 6672×1248 cells and is $32 \times 32\ \mu m^2$. In the gradient simulations, the simulation box measures $10\,000 \times 1872$ cells and is $48 \times 48\ \mu m^2$. In all simulations, the number of particles per cell was 20 for electrons, 8 for protons, and 12 for carbon. The time step was 15.4 as, to satisfy Courant's condition. In all simulations, the laser pulse had a wavelength of 0.8 μm, an intensity of 2×10^{18} W/cm^2, a duration of 30 fs, and a focal spot diameter of 10 μm. The laser pulse was focused onto the center of the front surface of the foil. The direction of propagation was 45° with respect to the target normal. To simplify the simulations, it was decided to make the laser propagate in the x_1 direction by rotating the target by 45°. In all simulations, the target was 10 μm thick and 30 μm wide. The peak target electron density was 10 times the critical density for the laser beam, i.e., 1.1×10^{22} cm^{-3}. The target ion composition was H^+ and C^{4+} in a ratio of 2:1. The target ion density was such that the entire target was charge neutral.

For the hard-edge target, the density profiles in the target normal and transverse directions were rectangular. The density profile for the gradient target was much like that of the hard-edge target, but with a density gradient at the front surface (facing the laser pulse). Radiation-hydrodynamic simulations of the pre-pulse interaction were performed using good approximations to the actual experimental parameters. This resulted in significant hydrodynamic expansion. The resulting density profile was fitted so that it could be mapped into a PIC code. The gradient extended for about 15 μm in the target normal direction, and the electron density rose linearly from 0 cm^{-3} to 1.1×10^{22} cm^{-3}, with matching ion densities. As discussed above, this density gradient mimics the plasma expansion due to preheating by the 2-ns pre-pulse.

The simulation results are shown in Fig. 4. For both simulations, (p_2, p_1) plots were produced at intervals of 185 fs for the total simulation duration of 2.78 ps. For the gradient target (with a pre-pulse), the results were significantly different. Most protons were emitted in the direction of the target normal, with numbers falling off for oblique angles. Protons emitted from the laser impact site appear to have the highest energies. The most energetic protons were emitted from two locations: the laser impact site and near the far edge of the target. Within proton bunches, there are clear correlations between the transverse position on the target from which they are emitted and their energy. For the hard-edge target (no pre-pulse), the phase space plots show that the protons were emitted from the target in all directions from multiple sources. The plots show that the protons have structures such as bunches, swirls, etc. When a structured proton beam enters the TPIS, one would expect that not all the protons would be on the same Thomson parabola, since the transverse position and angle at which they enter the TPIS varies with proton energy.

The classic Thomson parabola can be reproduced only if all protons enter the TPIS at the same angle and transverse position. In particular, the last few phase plots from the hard-edge target show a proton bunch being emitted with a strong correlation between proton speed and transverse position along the target. The difference in results between the two targets can be explained as follows. For the hard-edge target, the laser pulse cannot penetrate very far into the target. The pulse mostly heats the target electrons, which then expand and form a sheath. There is little interaction between the accelerated protons and the laser pulse.

For the gradient target, however, the laser pulse can penetrate the low-density plasma in front of the foil. A large fraction of the accelerated protons originate from the low-density gradient in front of the target,

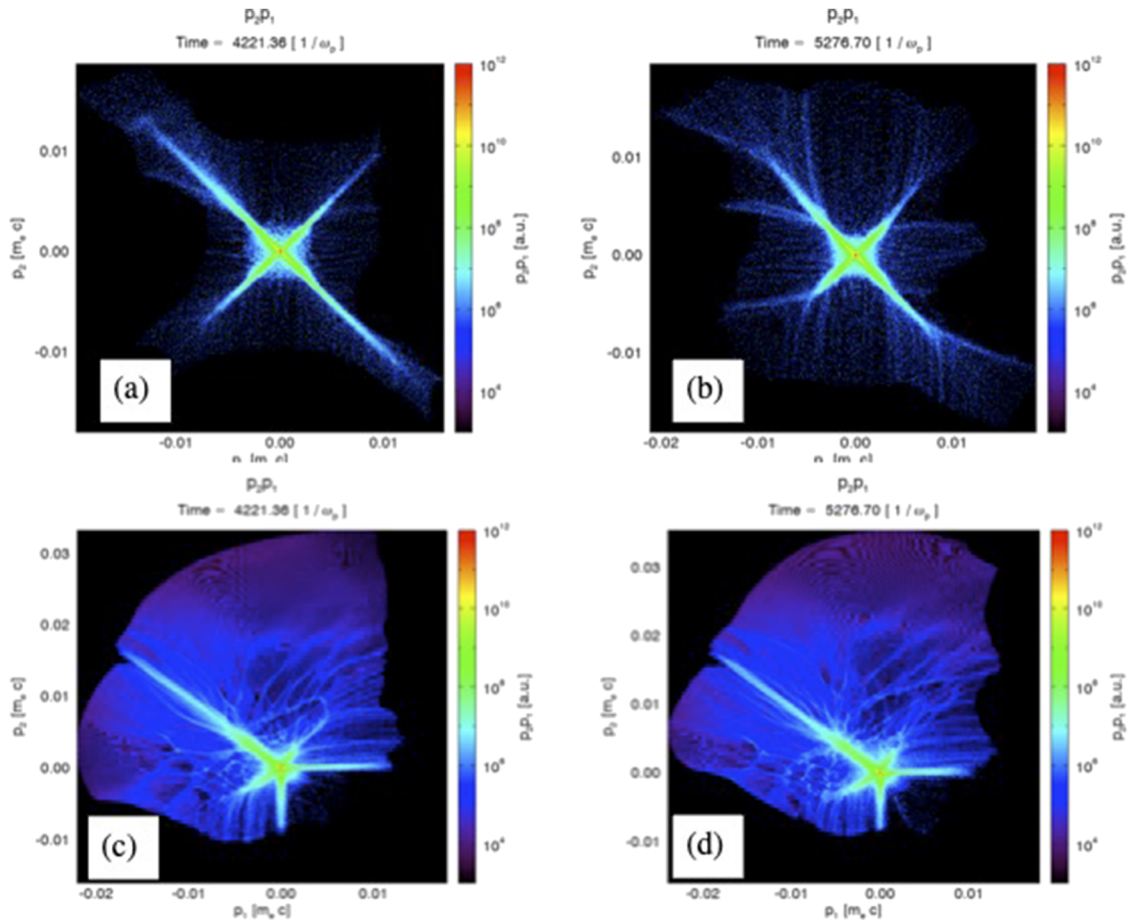

FIG. 4. Two-dimensional PIC simulation results. (p_2, p_1) plots of proton ions at various times: [(a) and (b)] without a pre-pulse and [(c) and (d)] with a pre-pulse.

rather than from the high-density interior part of the target. It is hypothesized that this interaction between the main laser pulse and the protons accelerated by the pre-pulse form a smooth sheath, and hence, there is an unperturbed source accelerated by the Coulomb force.

To understand the pointing of the laser-accelerated proton beams, it is very important to have a detailed understanding of the temporal evolution of the acceleration process. Our study can be further improved by using PIC simulations to understand the variation in the angular beam emittance and perturbation for the various targets described in this paper.

V. CONCLUSION

In conclusion, we studied the ion emission from the front surface of solid targets interacting with terawatt laser pulses. Our study indicates that proton emission from the target front surface is not uniform due to the perturbation in the source arising from intense laser plasma interactions. The wiggling of the beams was further characterized by using thick plastic targets. We found that the maximum source perturbation of protons occurred for plastic targets. We investigated a technique to control this by manipulating the laser parameters, specifically, by adding a proper pre-pulse to the main laser pulse. Two-dimensional PIC simulations were performed for the CH targets with and without pre-pulses. The simulations agree well with the experimental results. The introduction of a long pre-pulse smears out any perturbations of the ion source, resulting in a well-defined steering of the ion beam. This study could improve our understanding of ion acceleration and aid in using these directed proton beams for fast ignition fusion by depositing the maximum amount of energy in the core to produce viable fusion energy.

ACKNOWLEDGMENTS

B.R. acknowledges the funding support from the SERB Imprint Project No. IMP/2019/000275 and technical support from the laser team at the Raja Ramanna Centre for Advanced Technology.

REFERENCES

[1]R. A. Snavely, M. H. Key, S. P. Hatchett, T. E. Cowan, M. Roth *et al.*, "Intense high-energy proton beams from petawatt-laser irradiation of solids," Phys. Rev. Lett. **85**, 2945 (2000).

[2]A. Macchi, M. Borghesi, and M. Passoni, "Ion acceleration by superintense laser-plasma interaction," Rev. Mod. Phys. **85**, 751 (2013).
[3]J. Fuchs, P. Antici, E. d'Humières, E. Lefebvre, M. Borghesi *et al.*, "Laser-driven proton scaling laws and new paths towards energy increase," Nat. Phys. **2**, 48 (2006).
[4]T. Tajima and J. M. Dawson, "Laser electron accelerator," Phys. Rev. Lett. **43**, 267 (1979).
[5]M. Borghesi, S. Bulanov, D. H. Campbell, R. J. Clarke, T. Zh. Esirkepov *et al.*, "Macroscopic evidence of soliton formation in multiterawatt laser-plasma interaction," Phys. Rev. Lett. **88**, 135002 (2002).
[6]K. Quinn, P. A. Wilson, C. A. Cecchetti, B. Ramakrishna, L. Romagnani *et al.*, "Laser-driven ultrafast field propagation on solid surfaces," Phys. Rev. Lett. **102**, 194801 (2009).
[7]K. Quinn, P. A. Wilson, B. Ramakrishna, L. Romagnani, G. Sarri *et al.*, "Modified proton radiography arrangement for the detection of ultrafast field fronts," Rev. Sci. Instrum. **80**, 113506 (2009).
[8]S. V. Bulanov, T. Z. Esirkepov, V. S. Khoroshkov, A. V. Kuznetsov, and F. Pegoraro, "Oncological hadron therapy with laser ion accelerators," Phys. Lett. A **299**, 240 (2002).
[9]V. Malka, S. Fritzler, E. Lefebvre, E. d'Humières, R. Ferrand *et al.*, "Practicability of proton therapy using compact laser systems," Med. Phys. **31**, 1587 (2004).
[10]See http://www.isocorp.com for information about Radiochromic film detectors.
[11]See http://www.srim.org for proton stopping power calculations.
[12]M. Borghesi, A. J. Mackinnon, D. H. Campbell, D. G. Hicks, S. Kar *et al.*, "Multi-MeV proton source investigations in ultraintense laser-foil interactions," Phys. Rev. Lett. **92**, 055003 (2004).
[13]A. J. Mackinnon, P. K. Patel, M. Borghesi, R. C. Clarke, R. R. Freeman *et al.*, "Proton radiography of a laser-driven implosion," Phys. Rev. Lett. **97**, 045001 (2006).
[14]L. Romagnani, J. Fuchs, M. Borghesi, P. Antici, P. Audebert *et al.*, "Dynamics of electric fields driving the laser acceleration of multi-MeV protons," Phys. Rev. Lett. **95**, 195001 (2005).
[15]H. Schwoerer, S. Pfotenhauer, O. Jäckel, K.-U. Amthor, B. Liesfeld *et al.*, "Laser-plasma acceleration of quasi-monoenergetic protons from microstructured targets," Nature **439**, 445 (2006).
[16]S. M. Pfotenhauer, O. Jäckel, A. Sachtleben, J. Polz, W. Ziegler *et al.*, "Spectral shaping of laser generated proton beams," New J. Phys. **10**, 033034 (2008).
[17]B. Ramakrishna, M. Murakami, M. Borghesi, L. Ehrentraut, P. V. Nickles *et al.*, "Laser-driven quasimonoenergetic proton burst from water spray target," Phys. Plasmas **17**, 083113 (2010).
[18]T. E. Cowan, J. Fuchs, H. Ruhl, A. Kemp, P. Audebert *et al.*, "Ultralow emittance, multi-MeV proton beams from a laser virtual-cathode plasma accelerator," Phys. Rev. Lett. **92**, 204801 (2004).
[19]K. Ziel, J. Metzkes, T. Kluge, M. Bussmann, T. E. Cowan *et al.*, "Direct observation of prompt pre-thermal laser ion sheath acceleration," Nat. Commun. **3**, 874 (2012).
[20]J. Schreiber, S. Ter-Avetisyan, E. Risse, M. P. Kalachnikov, P. V. Nickles, W. Sandner, U. Schramm, D. Habs, J. Witte, and M. Schnürer, "Pointing of laser-accelerated proton beams," Phys. Plasmas **13**, 033111 (2006).
[21]J. Schreiber, M. Kaluza, F. Grüner, U. Schramm, B. M. Hegelich, J. Cobble, M. Geissler, E. Brambrink, J. Fuchs, P. Audebert, D. Habs, and K. Witte, "Source-size measurements and charge distributions of ions accelerated from thin foils irradiated by high-intensity laser pulse," Appl. Phys. B: Lasers Opt. **79**, 1041 (2004).
[22]S. Busch, M. Schnürer, M. Kalashnikov, H. Schönnagel, H. Stiel *et al.*, "Ion acceleration with ultrafast lasers," Appl. Phys. Lett. **82**, 3354 (2003).
[23]V. T. Tikhonchuk, A. A. Andreev, S. G. Bochkarev, V. Y. Bychenkov *et al.*, "Ion acceleration in short-laser-pulse interaction with solid foils," Plasma Phys. Controlled Fusion **47**(12B), B869–B877 (2005).
[24]A. P. L. Robinson, D. Neely, P. McKenna, and R. G. Evans, "Spectral control in proton acceleration with multiple laser pulses," Plasma Phys. Controlled Fusion **49**(4), 373–384 (2007).
[25]R. A. Fonseca, L. O. Silva, F. S. Tsung, V. K. Decyk, W. Lu *et al.*, "OSIRIS: A three-dimensional, fully relativistic particle in cell code for modeling plasma based accelerators," Lect. Notes Comput. Sci. **2331**, 342 (2002).